DOI: 10.1002/ejic.201101119

Synthesis and Structure of Silver Amino-Arenesulfonates

Madleen Busse,[a] Philip C. Andrews,*[a] and Peter C. Junk[a]

Keywords: Silver / Arenesulfonates / Zwitterions / Coordination polymers

Treatment of a variety of zwitterionic amino-arenesulfonic acids with silver oxide has resulted in the synthesis of seven new Ag^I amino-arenesulfonates $[Ag(O_3SR)]_\infty$ [R = *o*-aminobenzyl (*o*AB) (**1**), *m*-aminobenzyl (*m*AB) (**2**), 6-amino-3-methoxybenzyl (6A3MB) (**3**), *o*-aminonaphthyl (*o*AN) (**4**), 5-aminonaphthyl (5AN) (**5**), 4-amino-3-hydroxynaphthyl (4A3HN) (**6**) and 5-isoquinolinyl (I) (**7**)]. This has allowed an exploration of their coordination chemistry, whereby we examine the impact of structural diversity in the anions: the position of the amino functionality on the arene moiety, inclusion of the N within a heterocycle and an increase in ring size from phenyl to naphthyl. The solid-state structures of **1**, **2** and two forms of **4**, one with a coordinated water molecule, have been determined by X-ray diffraction and are all polymeric. Analytical data is provided for two of the structurally known complexes: known silver *p*-aminobenzenesulfonate **8** $[Ag(O_3SBA\textit{p})]_\infty$ and Ag^I 2-pyridinesulfonate $[Ag(O_3SP)]_\infty$ (**9**). The composition of all nine complexes has been confirmed through NMR spectroscopy, MS-ES$^+$, FTIR and elemental analysis.

Introduction

Interest in the medical and biological applications of silver metal and Ag^I complexes has grown substantially over the past decade.[1] Today they are present as antimicrobial agents in materials as diverse as topical creams for the treatment of burns (e.g., Ag^I sulfadiazine) and in immobilized polymer–silver membranes, which are now employed in a wide range of infection-resistant biomedical devices, coated medical instruments, wound dressings and in food-processing equipment.[1]

The incorporation of silver nanoparticles into polymeric membranes that contain sulfonated surfaces [e.g., sulfonated polyethersulfone (SPES)],[1c] polyvinyl sulfonate (PVS),[1h] styrene sulfonate polymers[1g] and even naturally available polysaccharides[1f] has proven to provide bactericidal properties against a range of different bacteria, including *Staphylococcus aureus*,[1c] *Staphylococcus albus*,[1c] *Staphylococcus epidermidis*,[1h] *Escherichia coli*[1c] and *Pseudomonas aeruginosa*.[1d]

Beyond polymers, Ag^I sulfonate complexes themselves have demonstrated potential application in selective and reversible guest inclusion,[2] especially when the metal–organic complexes incorporate neutral N-containing secondary ligands,[2g,2h,2k,3] whereas arenesulfonates have found commercial application in the cosmetics industry as hair dying agents[4] and in the laser and thermal printing industry.[5]

Surprising is the fact that the majority of these applications have been developed only recently. Until around the beginning of this century, the coordination chemistry of sulfonates was not well investigated or understood, the change being marked by a series of papers by Côté and Shimizu et al.,[2a,2b,2d–2f,6] Cai et al.[7] and others,[8] by investigating metal sulfonates as a family of layered solids. The former lack of activity most likely derives from our understanding that the monoanionic sulfonate group is generally a weaker coordinating ligand than other acidato anions such as carbonates or phosphonates,[6e–6g,9] often rendering the sulfonate ligand incapable of forming functional extended solids. However, ligands that allow flexibility in their binding modes to metal centres have become more sought after, and the number of coordination solids that incorporate them in a variety of bonding modes and motifs has continued to increase over the past few years.[7a,10]

Systematic studies of Ag^I arenesulfonates have previously been undertaken by Côté and Shimizu et al.,[2b] and more recently by Zhu and Gao et al.[11] The former study charts the influence of an increase in the size of the ring system on observed structural outcomes, whereas in the latter, *o*-hydroxy arenesulfonic acids, which contain one or more $-SO_3H$ groups positioned at various points on a single phenyl ring, are used to provide a diverse range of supramolecular frameworks.

Our current investigations represent the first systematic study of the coordination chemistry of Ag^I amino-arenesulfonates. In choosing the range of amino-arenesulfonic acids, four key structural factors were considered important: (i) the position of the amino group on the arene moiety would be varied from *ortho* to *meta* to *para*; (ii) heterocyclic amines would be studied to increase structural diver-

[a] School of Chemistry, Monash University,
Melbourne, 3800 VIC, Australia
Fax: +61-3-9905-4597
E-mail: phil.andrews@monash.edu

sity and to act as comparators with the exocyclic amines; (iii) the acids would be monoprotic zwitterions; and (iv) ring size would be varied from phenyl to naphthyl.

From this study we now report the synthesis and characterization of seven new Ag^I amino-arenesulfonates $[Ag(O_3SR)]_\infty$ [R = *o*-aminobenzyl (*o*AB) (**1**), *m*-aminobenzyl (*m*AB) (**2**), 6-amino-3-methoxybenzyl (6A3MB) (**3**), *o*-aminonaphthyl (*o*AN) (**4**), 5-aminonaphthyl (5AN) (**5**), 4-amino-3-hydroxynaphthyl (4A3HN) (**6**) and 5-isoquinolinyl (I) (**7**)]. The acids are shown in Scheme 1.

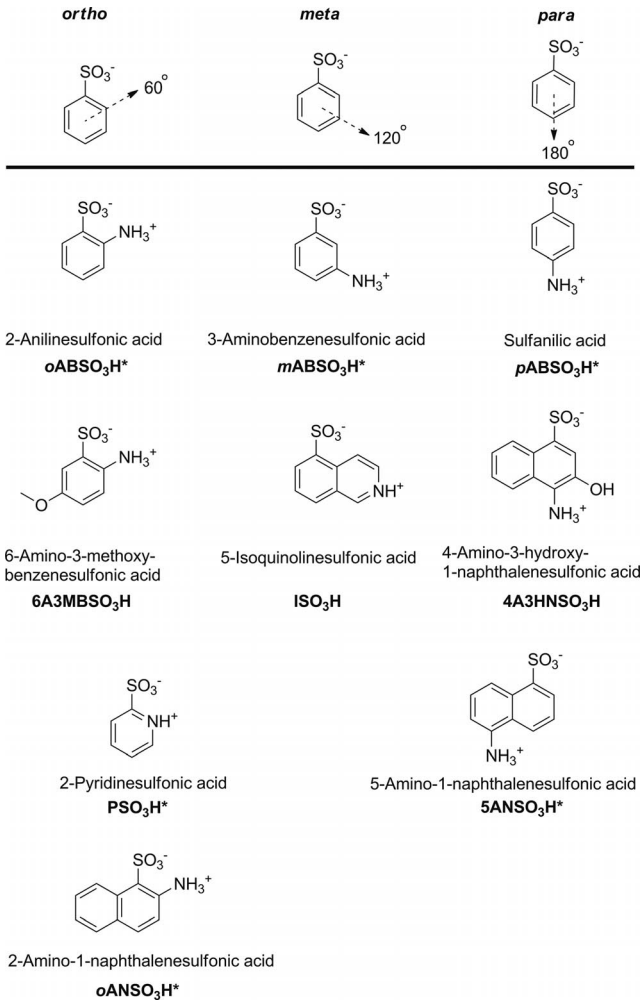

Scheme 1. Structures of the aminosulfonic acid ligands applied in the synthesis of the Ag^I amino-arenesulfonates. X-ray structures were obtained for those structures labelled with asterisks (*).

Possible coordination modes of the *o*-aminobenzenesulfonate ligand involving the amino functionality are shown in Scheme 2 (only one type or a combination of these displayed). The solid-state structures of complexes **1**, **2**, **4a** and **4b** have been determined by single-crystal X-ray diffraction, and we provide further analytical data for the known silver *p*-aminobenzenesulfonate[12] $[Ag(O_3SBAp)]_\infty$ **8** and Ag^I 2-pyridinesulfonate[2i] $[Ag(O_3SP)]_\infty$ **9**, since only structural information has been reported thus far.

Results and Discussion

Synthesis

Target compounds **1**–**9** were all synthesized from the appropriate sulfonic acid and freshly prepared Ag_2O[13] in water at 90 °C by using the stoichiometric ratio of 2:1 (Scheme 3). Crystalline material suitable for single-crystal X-ray diffraction studies was obtained through very slow cooling of the homogeneous solution in a water bath to room temperature for complexes **1**, **2** and **4a**, and for **4b** through recrystallization in a small amount of ethanol. All the Ag^I complexes **1**–**9** were characterized through ^1H and ^{13}C NMR spectroscopy, FTIR and MS-ES$^+$. Elemental analysis and melting-point determination were also performed.

$$Ag_2O + 2\,RSO_3H \xrightarrow[120\ min]{H_2O\ (90\ °C)} 2\,[Ag(O_3SR)] + H_2O$$

Scheme 3. General reaction scheme of the synthesis of $[Ag(O_3SR)]_\infty$ [R = *o*-aminobenzyl (*o*AB) (**1**), *m*-aminobenzyl (*m*AB) (**2**), 6-amino-3-methoxybenzyl (6A3MB) (**3**), *o*-aminonaphthyl (*o*AN) (**4**), 5-aminonaphthyl (5AN) (**5**), 4-amino-3-hydroxynaphthyl (4A3HN) (**6**), 5-isoquinolinyl (I) (**7**), *p*-aminobenzyl (*p*AB) (**8**) and 2-pyridyl (P) (**9**)].

X-ray Crystallographic Studies

$[Ag(O_3SBA_o)]_\infty$ (1)

Compound **1** is represented by a 1D chain growing along the crystallographic *c* axis (Figure 1). A summary of bond lengths and angles is given in Table 1. In each chain only one type of Ag^I centre is present and has a pseudo-tetrahedral coordination geometry composed of two sulfonate oxygen atoms, the nitrogen atom and two aromatic carbon

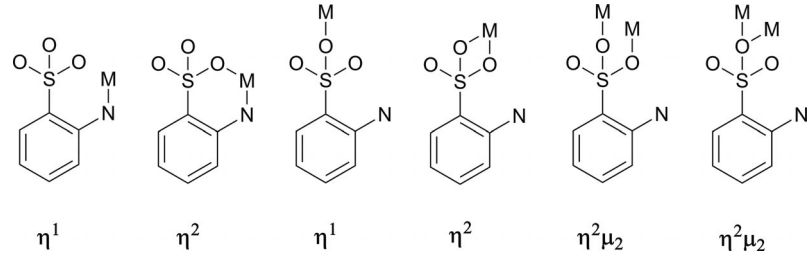

Scheme 2. Possible coordination modes shown for the *o*-aminobenzenesulfonate ligand in the solid-state involving the amino group in bonding to the metal ion.

atoms. This differs from the previously described 2-pyridinesulfonate analogue **9**,[2i] in which the polymeric structure forms a 2D network with one type of silver centre in an asymmetrical trigonal-bipyramidal coordination geometry. The trigonal basis of the trigonal bipyramid is composed of two sulfonate oxygen atoms in a μ_4 [μ_2O(1) and μ_2O(3)] bridging mode; the apices are occupied by one sulfonate oxygen atom and the pyridyl nitrogen atom. Therefore, the 2-pyridinesulfonate ligand stabilizes the molecular scaffold by linking four metal centres.[2i] Another key difference is the η^2 interaction of the Ph ring with the Ag centre, which is apparent in **1** but not in **9**.

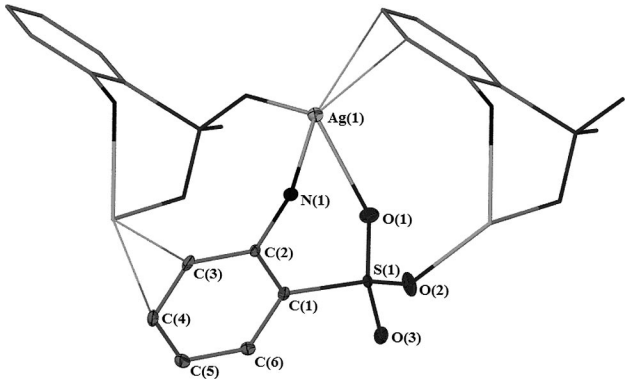

Figure 1. Structure of $[Ag(O_3SBA\textit{o})]_\infty$ (**1**). View of an individual 1D polymeric chain growing along the crystallographic *c* axis showing the connectivity modes observed of the amino-arenesulfonate ligand to the Ag^I centre. Hydrogen atoms are omitted for clarity. Ellipsoids are shown at 50% probability.

In contrast to **9**, compound **1** possesses a μ_2 [κ^2-*O*(1),*O*(2)] coordination mode for the sulfonate group [Ag(1)–O(1), 2.496(3) Å; Ag(1)–O(2′), 2.335(3) Å (′ = *x*, –1/2 – *y*, *z* – 1/2)] and a κ*N* bridge for the NH_2 group [Ag(1)–N(1), 2.321(4) Å]. Thus, one *o*-aminobenzenesulfonate ligand is capable of connecting to three Ag^I centres in an overall μ_2:η^3 coordination mode. No bridging sulfonate oxygen atoms are observed in **1** and therefore no extended network is formed. As might be expected with the amino group in the *ortho* position, the Ag^I centre is chelated by one sulfonate oxygen atom and the nitrogen atom to form a boat-shaped six-membered ring. The arene moiety forms a weak electrostatic interaction with the silver centre, thereby establishing an η^2 coordination mode from the 3,4-positions of the ring [Ag(1)–C(3′), 2.521(4) Å; Ag(1)–C(4′), 2.502(4) Å (′ = *x*, –1/2 – *y*, 1/2 – *z*)]. The interaction places the phenyl ring perpendicular to the Ag^I centre [Ag(1)–C(1)–C(4), 90.0(7)°] as the sulfur atom of the sulfonate group holds on to its almost perfect tetrahedral geometry. The packing of the 1D chains results in a 3D network in which the individual 1D chains are connected through hydrogen-bonding interactions along the crystallographic *a* axis (Figure 2), whereas π-stacking (face-to-face) interactions are observed along the crystallographic *b* axis. The 2-pyridinesulfonate analogue **9** shows a perpendicular arrangement of the phenyl rings along the crystallographic *c*

Table 1. Selected bond lengths [Å] and angles [°] of compounds **1**, **2**, **4a** and **4b**. Symmetry operators: **1** (′ = *x*, –*y* – 1/2, *z* – 1/2); **2** (′ = –*x* + 1/2 – *y*, *z* + 1/2, ′′ = *x* + 1/2, –*y* + 1/2, –*z*); **3** (′ = –*x*, *y* + 1/2, –*z*); **4** (′ = –*x*, –*y*, –*z*, ′′ = *x* + 1/2, –*y* + 1/2, *z* – 1/2).

1							
Ag(1)–N(1)	2.324(3)	S(1)–O(3)	1.456(2)	N(1)–Ag(1)–O(2′)	122.65(10)	O(3)–S(1)–O(2)	113.22(15)
Ag(1)–O(2′)	2.336(2)	S(1)–O(2)	1.457(2)	N(1)–Ag(1)–O(1)	80.54(9)	O(3)–S(1)–O(1)	112.27(14)
Ag(1)–O(1)	2.497(3)	S(1)–O(1)	1.459(2)	O(2′)–Ag(1)–O(1)	93.54(9)	O(2)–S(1)–O(1)	112.70(16)
Ag(1)–C(4′)	2.501(3)	N(1)–C(2)	1.416(4)	S(1)–O(2′)–Ag(1)	142.12(17)		
Ag(1)–C(3′)	2.522(3)			S(1)–O(1)–Ag(1)	121.71(13)		
2							
Ag(1)–N(1′)	2.2402(18)	S(1)–O(3)	1.4504(14)	N(1′)–Ag(1)–O(2)	142.19(6)	O(3)–S(1)–O(2)	113.84(9)
Ag(1)–O(2)	2.2957(13)	S(1)–O(2)	1.4557(16)	N(1′)–Ag(1)–O(1′′)	126.21(6)	O(3)–S(1)–O(1)	111.92(8)
Ag(1)–O(1′′)	2.3719(15)	S(1)–O(1)	1.4678(15)	O(2)–Ag(1)–O(1′′)	88.46(5)	O(2)–S(1)–O(1)	111.64(9)
Ag(1)–O(1)	2.5168(14)	N(1)–C(3)	1.417(2)	N(1′)–Ag(1)–O(1)	93.31(6)		
				O(2)–Ag(1)–O(1)	94.42(5)		
				Ag(1′′)–O(1)–Ag(1)	111.34(5)		
4a							
Ag(1)–N(1)	2.320(6)	S(1)–O(3)	1.461(5)	N(1)–Ag(1)–O(1)	125.3(2)	O(3)–S(1)–O(2)	114.4(3)
Ag(1)–O(1)	2.385(6)	S(1)–O(2)	1.472(5)	N(1)–Ag(1)–O(4)	86.9(2)	O(3)–S(1)–O(1)	111.8(3)
Ag(1)–O(4)	2.397(5)	S(1)–O(1)	1.478(6)	O(1)–Ag(1)–O(4)	106.7(2)	O(2)–S(1)–O(1)	110.4(4)
Ag(1)–C(6′)	2.485(6)	S(2)–O(1)	1.462(5)	N(1)–Ag(1)-C(7′)	108.6(2)		
Ag(1)–C(7′)	2.464(7)	S(2)–O(3)	1.480(6)	S(1)–O(1)–Ag(1)	116.0(3)		
		C(2)–N(1)	1.397(8)				
4b							
Ag(1)–N(1′)	2.2829(16)	S(1)–O(3)	1.4447(14)	N(1′)–Ag(1)–O(2′)	127.95(5)	O(3)–S(1)–O(1)	113.35(9)
Ag(1)–O(2′)	2.422(14)	S(1)–O(1)	1.4540(14)	N(1′)–Ag(1)–O(1)	113.15(5)	O(3)–S(1)–O(2)	111.09(8)
Ag(1)–O(1)	2.4493(18)	S(1)–O(2)	1.4658(13)	O(2′)–Ag(1)–O(1)	101.31(4)	O(1)–S(1)–O(2)	110.97(8)
Ag(1)–C(6′′)	2.5427(19)			S(1)–O(1)–Ag(1)	125.61(8)		
Ag(1)–C(7′′)	2.5615(17)			S(1)–O(2′)–Ag(1)	109.90(7)		

axis to result in T-shaped C–H/π interactions between the sheets (distance 3.698 Å). As the amino functionality is part of the pyridyl ring, no hydrogen bonding is observed in **9**.

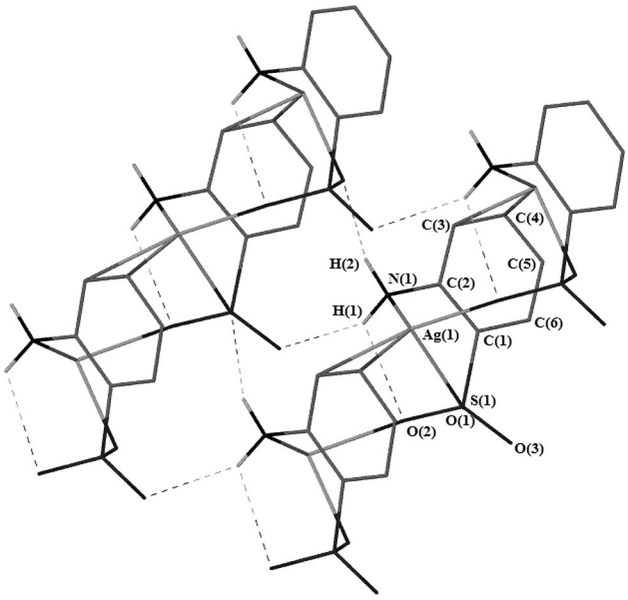

Figure 2. Hydrogen-bonding network of **1**. Only hydrogen atoms involved in hydrogen-bonding interactions are shown.

[Ag(O$_3$SBA$_m$)]$_\infty$ (2)

Shifting the amino group to the *meta* position results in complex **2**, which forms a 3D network in the solid state. The amino group and one oxygen atom of the sulfonate group allow the network to grow along the crystallographic *c* axis, whereas bridging through the second and third sulfonate oxygen atoms allows growth along the divergent crystallographic *a* and *b* axes. Only one type of Ag^I centre is present and again shows pseudo-tetrahedral geometry. However, one Ag^I centre is connected to four individual *m*-aminobenzenesulfonate ligands to exhibit an overall μ_4:η^4 coordination mode (Figure 3). The pyridyl complex [Ag(3-pySO$_3$)]$_\infty$, previously described by Mäkinen and Shimizu et al.,[2d] also forms a 3D network that consists of Ag^I ribbons growing along the crystallographic *c* axis. However, this compound accommodates two types of Ag^I ions, analogous to those previously observed in the Ag^I 2-pyridinesulfonate analogue **9**.[2i] In [Ag(3-pySO$_3$)]$_\infty$ only one metal centre is bound to sulfonate oxygen atoms, whereas the other binds through the third sulfonate oxygen atom and the pyridyl nitrogen atom.

As might be expected for this family of compounds, the amino group of **2** engages in a κ*N* bridge to the Ag^I centre [Ag(1)–N(1′), 2.241(2) Å (′ = 1/2 – *x*, –*y*, 1/2 + *z*)] and forms the shortest Ag–N bond of all the complexes **1**, **4a** and **4b** (see below). A summary of bond lengths and angles is given in Table 1. The sulfonate group adopts a μ_3:η^3 coordination mode [κ^2*O(1)* and κ*O(2)*]. The oxygen atom O(1) bridges two Ag^I centres thereby showing two different Ag–O bonds [O(1′′)–Ag(1), 2.3719(15) Å (′′ = *x* + 1/2, 1/2 – *y*, –*z*), O(1′′′)–Ag(1), 2.5168(14) Å (′′′ = *x*,*y*,*z*)], whereas

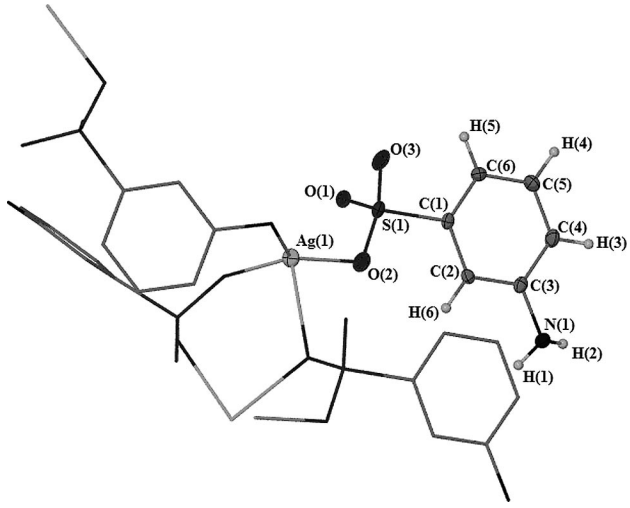

Figure 3. Structure of [Ag(O$_3$SBA*m*)]$_\infty$ (**2**). A 3D network is obtained for compound **2** as the amino group in the *meta* position on the ring and one oxygen atom of the sulfonate group allow growth of the network along the crystallographic *c* axis, whereas bridging through sulfonate oxygen atoms allows growth along the crystallographic *a* and *b* axes. Hydrogen atoms of the asymmetric unit are displayed. Ellipsoids are shown at 50% probability.

the bond to O(2) is the shortest at 2.2957(13) Å. The bridge angle for O(1) is 111.35(6)°. As in **1** (and in **4b**), the O(3) atom is not involved in any bonding with the Ag^I centres. Instead it bridges two hydrogen bonds [O(3′′′′)···H1–N(1), 2.34(3) Å (′′′′ = –*x*, *y* + 1/2 –*z* + 1/2), O(3′)···H(2)–N(1), 2.08(3) Å (′ = –*x* + 1/2, –*y*, *z* + 1/2)], which further enhances the stability of the network along the crystallographic *a*

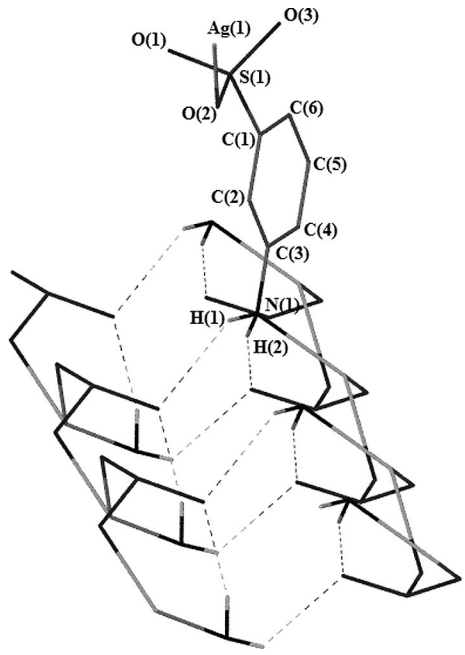

Figure 4. Display of the hydrogen bonds bridged by O(3) of the sulfonate group, which further enhances the stability of the network of **2** along the crystallographic *a* axis; the hydrogen bonds of one repeating unit show the motif of an *R*-helix winding down the crystallographic *a* axis.

axis; the hydrogen bonds of one repeating unit show the motif of an *R* helix winding down the crystallographic *a* axis (Figure 4). The phenyl group in **2** packs in a classical herringbone motif (also seen in **4b** below) that shows an array of nonclassical C–H/π-stacking interactions along the two crystallographic axes defined by the face-to-edge contacts of the phenyl ring.

[Ag(O$_3$SNA$_o$)(H$_2$O)]$_\infty$ (4a)

It is known that Ag^I *mono*-sulfonates will generally form anhydrous solids even when synthesized and isolated from aqueous solutions.[2b] There are rare exceptions to this and compound **4a** is one. The crystal structure shows one water molecule binding directly to the metal centre. This phenomenon was first observed in [Ag(H$_2$O)$_{0.5}$(1-naphthylenesulfonate)]$_\infty$[2b] and was ascribed to the increased length of the naphthyl moiety. The increased intramolecular space created by the naphthyl group also allows **4a** to retain the structural motif of the 1D chain, as adopted by the Ph analogue **1**. Bridging water molecules are thus incorporated into the polymeric chain (Figure 5), thus saturating the coordination environment of the Ag^I centre.

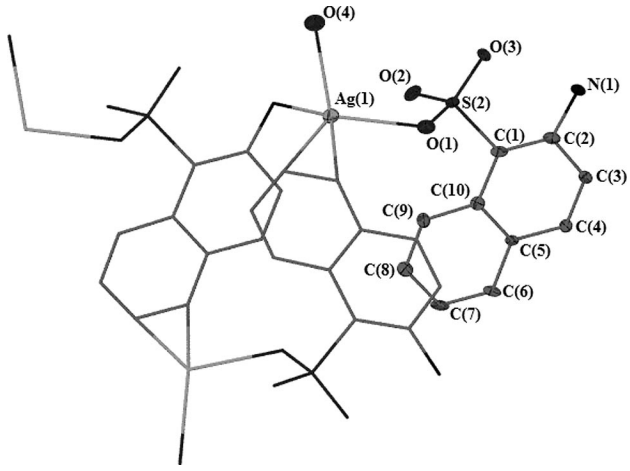

Figure 5. Structure of [Ag(O$_3$SNA*o*)(H$_2$O)]$_\infty$ (**4a**). View of an individual 1D polymeric chain growing along the crystallographic *b* axis showing the connectivity modes observed of the amino-arenesulfonate ligand to the unique Ag^I centre. Hydrogen atoms are omitted for clarity. Ellipsoids are shown at 50% probability.

As in **1**, the 1D chain in **4a** grows along the crystallographic *b* axis. In turn, only one unique Ag^I centre is again present and once more displays pseudo-tetrahedral coordination geometry. However, significant differences in the connectivity are seen due to the much more expanded structure (Figure 3). A summary of the bond lengths and angles is given in Table 1. Here only O(1) of the sulfonate group [Ag(1)–O(1), 2.383(6) Å] is involved in bonding to the metal centre. The sulfonate and amino groups show no chelation to any Ag^I centre. Instead the nitrogen atom bridges to a second Ag^I centre [Ag(1)–N(1′), 2.320(6) (′ = *x*, *y*, *z*)]. The Ag^I centre is again involved in π bonding to the arene moiety (Figure 6), but here the interaction is established with the more distant phenyl ring rather than that which contains the sulfonate moiety [Ag(1)–C(6′′), 2.464(7) Å; Ag(1)–C(7′′), 2.467(7) Å (′′ = –*x*, 1/2 + *y*, –*z*)]. On account of this coordination environment, the ligand is locked into place as the naphthyl moiety is perpendicular to the sulfonate group [S(1)–C(1)–C(9), 89.5(2)°] and the η^2 coordination mode from the 6,7-positions of the ring to the silver centre is fixed by a mean angle of 109.2(8)°. The coordination sphere of the silver centre is completed by an auxiliary ligation to one water molecule [Ag(1)–O(4), 2.397(5) Å] that points to the left and right of the chain.

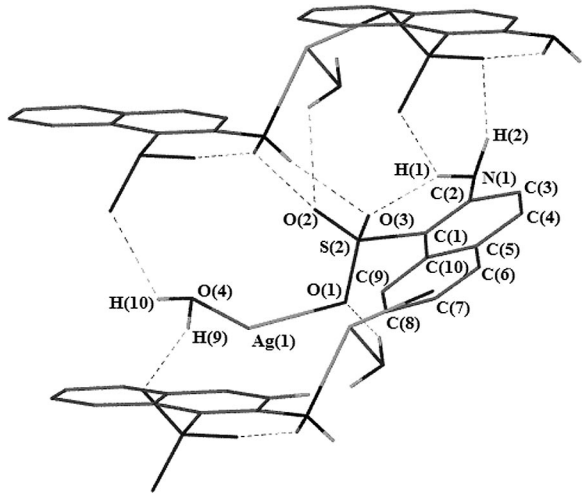

Figure 6. Hydrogen-bonding network of **4a**. The two sulfonate oxygen atoms that are not involved in the direct bonding to the metal centre play a significant role in intermolecular hydrogen bonding between the 1D chains; they are connected along the crystallographic *a* axis. An intramolecular hydrogen bond is observed for O(3) as a secondary interaction seen within one chain.

Looking down the crystallographic *a* axis, a zigzag pattern occurs similar to that observed in **1**. The two individual silver(I) chains are orientated exactly opposite to each other with respect to the arene moiety and its functional groups. The zigzag angle at the silver centre is 62.1(3)°. This facilitates a perfect alignment of the naphthyl rings to allow T-shaped C–H/π interactions (face-to-edge) with a distance of 3.581 Å. These interactions are also present between individual chains, which results in an overall classical herringbone motif along the crystallographic *c* axis, as reported for simple aromatic hydrocarbons,[14] naphthalene itself[12e] and its Ag^I arenesulfonate analogue.[2b] The two sulfonate oxygen atoms that are not involved in bonding to the metal centre play a significant role in intermolecular hydrogen bonding between the 1D chains; two originate from the water molecule [O(1′′)···H(9)–O(4), 2.040(8) Å, O(2′′)···H(10)–O(4), 2.390(15) Å (′′ = –*x*, 1/2 + *y*, –*z*)] and two from the amino functionality [O(2′′)···H(1)–N(1), 2.55 Å, O(3′′)···H(2)–N(1), 2.36 Å (′′ = –*x*, 1/2 + *y*, –*z*)]; and connect them along the crystallographic *a* axis (Figure 6). Another intramolecular hydrogen bond is observed for O(3) [O(3)···H(1)–N(1), 1.88 Å] as a secondary interaction within one chain (Figure 6).

{[Ag(O$_3$SNA$_o$)]·H$_2$O}$_\infty$ (4b)

In attempting to generate the anhydrous analogue of **4a**, crystals of **4a** were dissolved in ethanol and recrystallized. The result was complex **4b**, which retains a water molecule in the crystal lattice but not directly bound to the Ag^I centre. The absence of water bridging to the silver centre allows the formation of a 2D network that grows along the crystallographic *b* axis. The overall pseudo-tetrahedral geometry of the unique metal centre similar to that seen in **4a** (and in **1**) is maintained. As in compound **1**, two sulfonate oxygen atoms coordinate to the Ag^I centre along with the nitrogen atom and two aromatic carbon atoms. In contrast to **1**, however, the formation of a 2D network and the accommodation of the naphthyl moiety do not allow the chelation of the ligand to the metal centre. Therefore, in **4b** an overall coordination mode of μ_3:η^3 to three independent Ag^I centres is present [Ag(1)–N(1′), 2.2830(2) Å; Ag(1)–O(1), 2.450(2) Å; and Ag(1)–O(2′), 2.4230(2) Å (′ = –*x*, –*y*, –*z*)]. To maintain the pseudo-tetrahedral geometry around the Ag^I centre, the arene moiety coordinates in an η^2 mode from the 6,7-positions of the ring [Ag(1)–C6′′, 2.5620(2) Å; Ag(1)–C7′′, 2.5620(2) Å (′′ = 1/2 + *x*, 1/2 – *y*, 1/2 + *z*)]. Again O(3) of the sulfonate group is not involved in bonding to the Ag^I centre (Figure 7).

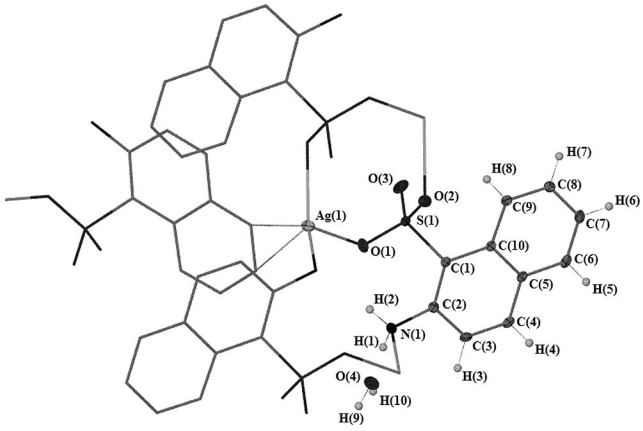

Figure 7. Structure of {[Ag(O$_3$SNA*o*)]·(H$_2$O)}$_\infty$ (**4b**). Connectivity of compound **4b** is shown with μ_3:η^3 coordination mode to three independent Ag^I centres. Hydrogen atoms of the asymmetric unit are shown. Ellipsoids are shown at 50% probability.

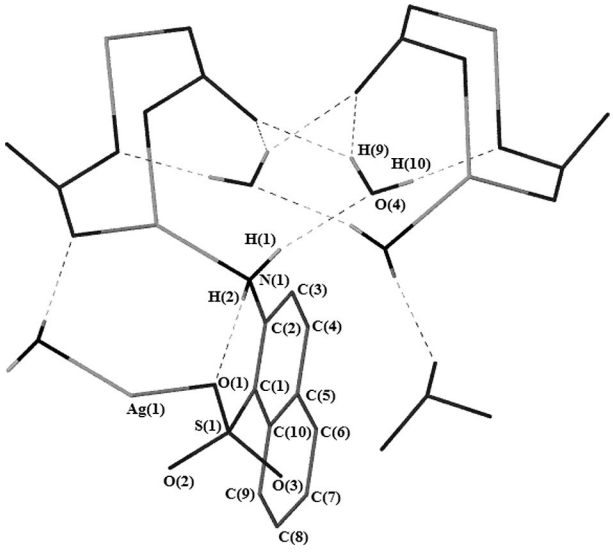

Figure 8. Hydrogen-bonding network of **4b**. Only hydrogen atoms involved in hydrogen-bonding interactions are shown.

A summary of bond lengths and angles for **4b** is given in Table 1. Five hydrogen bonds are observed within the structure (Figure 8): two derived from the amino group [O(1)···H2–N(1), 1.990(2) Å, O4···H1–N(1), 2.250(2) Å] and three from the water molecule that are present in the lattice [O(3)···H9–O4, 2.2400(2) Å, O(3′)···H9–O4, 2.4500(2) Å (′ = –*x*, *y*, –*z* + 1/2) and O(2′)′···H10–O4, 1.9900(2) Å (′′ = *x*, –*y*, *z* – 1/2)]. Compound **4b** is assigned as an anhydrous Ag^I amino-arenesulfonate as the coordination geometry around the Ag^I centre is exclusively made up of the ligand and does not include the water molecule.

Characterization

Complexes **1**–**9** and the starting acids were all studied by NMR spectroscopy in D_2O and/or [D_6]DMSO. In the ^{1}H NMR spectra the acids show the acidic proton as a broad singlet with chemical shift values in the range δ = 7–9 ppm. Upon deprotonation and complexation with Ag^I, this signal disappears thereby confirming formation of the ligand and the corresponding silver compounds. In comparison with the free acids, upon complexation the ^{13}C NMR spectra show low-frequency shifts for the resonance that corresponds to the quaternary carbon *C*-(SO$_3$Ag) by between

Table 2. Observed coordination modes for Ag^I to the sulfonate group and the assignment of the corresponding absorption bands.

	$\tilde{\nu}$(NH$_2$)[a]	$\tilde{\nu}$(SO$_3$)[a]	CM[b]	CS[c]
*o*ABSO$_3$H	3418	1228, 1204, 1027		
1	3320, 3257	1204, 1174, 1013	μ_2:η^3	x
*m*ABSO$_3$H	3437	1208, 1101, 1026		
2	3362, 3246	1210, 1147, 1108, 1027	μ_4:η^4	x
6A3MBSO$_3$H	3391	1260, 1187, 1024		
3	3336, 3070	1253, 1186, 1134, 1023		
*o*ANBSO$_3$H	3470	1242, 1182, 1045		
4a	3433, 3342	1193, 1050	μ_2:η^2	x
4b	3412, 3341	1158, 1029	μ_3:η^3	x
5ANSO$_3$H	3421	1226, 1170, 1057		
5	3401, 3348	1167, 1027		
3H4ASO$_3$H	3239	1218, 1169, 1048		
6	3159, 3078	1197, 1157, 1042		
ISO$_3$H	3429	1215, 1198, 1052		
7	3437, 3351	1210, 1175, 1056		
*p*ABSO$_3$H	3418	1245, 1156, 1033		
8	3319, 3266	1249, 1186, 1153, 1123	μ_4:η^4	x[d]
PSO$_3$H	–	1269, 1148, 1039		
9	–	1207, 1165, 1146, 1019	μ_5:η^5	x[e]

[a] FTIR absorption bands are taken from the Nujol spectra [cm^{-1}]. [b] CM = coordination mode. CM assigned in red were confirmed through X-ray crystallography. [c] CS = crystal structure. Overall CM was confirmed through X-ray crystallography. [d] Crystal structure is known in the literature of compound [Ag(2-pySO$_3$)]$_\infty$.[2i] [e] Crystal structure is known in the literature of compound [Ag(O$_3$SBA*p*)]$_\infty$.[12a–12d]

3 and 5 ppm. Full details of the chemical shifts and their assignments for **1**–**9** are given in the Experimental Section.

FTIR spectra visualize the different coordination modes of the silver metal to the sulfonic acid group by showing the appropriate number of absorption bands. A bathochromic shift for the amino absorption band is ascribed to the coordination of the amino functionality to the Ag^I centre. The sulfonate group shows a range of absorption bands in the region 1200–1000 cm^{-1} according to the coordination mode this functional group displays within the solid-state structure. The coordination modes for **1**, **2**, **4a**, **4b**, **8** and **9** have been established through crystallography and as such their coordination mode is known. Table 2 summarizes the main features observed in FTIR spectroscopy and the observed bonding modes of the sulfonato ligands. However, too little data currently exists to allow the binding and coordination of the other complexes to be predicted based on the IR spectroscopic data alone.

Mass spectrometry provided unambiguous evidence for silver complexes **1**–**9** to be arranged as polymeric structures. In the case of the *p*-aminobenzenesulfonate, two quartets (1/3/3/1) at 665/667/669/671 $[Ag_3\mathbf{L}_2]^+$ and 743/745/747/749 $[Ag_3\mathbf{L}_2(DMSO)]^+$ and a quintet (1/4/6/4/1) at 944/946/948/950/952 $[Ag_4\mathbf{L}_3]^+$ were observed underlining the polymeric nature of the silver compound **8**. A summary of the common ions detected for all the structures can be found in Table 3.

Table 3. Summary of common ions detected in mass spectra for compounds **1**–**9**.

	$\mathbf{L}^-$	$[Ag\mathbf{L} + Na]^+$	$[Ag\mathbf{L}(s) + Na]^+$	$[Ag_2\mathbf{L}]^+$	$[Ag_2\mathbf{L}(s)]^+$
1	*o*$ABSO_3$			386/388/390	464/466/468[b]
2	*m*$ABSO_3$	302/304		386/388/390	464/466/468[b]
3	6A3MBSO$_3$	332/334			
4a	*o*$ANSO_3$			436/438/440	520/522/524[c]
5	5$ANSO_3$			436/438/440	
6	3H4ANSO$_3$	368/370			470/472/474[a]
7	ISO_3		356/358[a]		
8	*p*$ABSO_3$				464/466/468[b]
					542/544/546[b]*
9	PSO_3			372/374/376	456/458/460[c]

[a] Solvent H_2O. [b] Solvent DMSO or * $(DMSO)_2$. [c] Solvent dichloromethane.

Conclusion

We have described the synthesis and characterization of seven new Ag^I amino-arenesulfonates and a systematic study on their coordination chemistry. Mass spectroscopic data indicate the compounds to be polymeric in nature and are supported by those complexes **1**, **2**, **4a** and **4b** that have been confirmed by single-crystal X-ray diffraction. Structural changes in the position of the amino functionality on the arene moiety from *ortho* to *meta* to *para*, the increase in ring size from a phenyl to a naphthyl moiety and inclusion of the N atom in a heterocycle all impact directly on the adopted structures. All presented structures have a unique silver ion incorporated that displays pseudo-tetrahedral geometry. This phenomenon of having a unique Ag^I centre is in contrast to the reported pyridyl analogues, which consist of two geometrically different Ag^I centres. Despite being synthesized in water, anhydrous compounds were obtained for all compounds **1**–**9**. An exception is the *o*-aminonaphthalenesulfonate ligand **4a**, which results in a hydrated solid structure with one water molecule bound directly to the Ag centre. Recrystallization from ethanol yielded the anhydrous compound.

We are currently exploring the antimicrobial properties of these compounds for use in medical applications (see Introduction) and assessing their potential as precursors to new metal sulfonates through metathesis, especially when the zwitterionic nature of the aminosulfonate inhibits direct complex formation.

Experimental Section

General Considerations: All sulfonic acids were purchased from Aldrich Chemical Co. Ag_2O was freshly synthesized according to Tanabe and Peters.[13] Infrared spectra were obtained with a Perkin–Elmer 1600 FTIR spectrometer. NMR spectra were obtained with Bruker AV300 or AV400 spectrometers with chemical shifts referenced to $[D_6]$DMSO or D_2O. Electrospray ionization mass spectrometry (ESI-MS) was performed with a Micromass Platform electrospray mass spectrometer. Elemental analysis (EA) was performed by The Campbell Microanalytical Laboratory, Department of Chemistry, University of Otago, New Zealand. Melting points are uncalibrated and were determined with a Bibby Stuart Scientific melting-point apparatus SMP3.

Synthesis, General Procedure: The individual sulfonic acid (2 mmol, 2 equiv.) was dissolved in water (50 mL) and the temperature was set to 90 °C. Fresh Ag_2O (1 mmol, 1 equiv.) was added to this solution, and the reaction mixture was stirred for 2 h. The solution was filtered hot and the filtrate was kept in a water bath at 50 °C overnight. The filtrate was allowed to cool to room temperature very slowly to yield the desired product either as crystalline material (**1**, **2**, **4a**, **4b**, **8** and **9**) or as an amorphous powder (**3**, **5**–**7**).

$[Ag(O_3SBAo)]_\infty$ (1): The general procedure was followed using *o*-aminobenzenesulfonic acid to yield pink crystalline needles (269 mg, 96%) suitable for X-ray crystallography; m.p. > 250 °C (decomp.). ^1H NMR (300 MHz, $[D_6]$DMSO, 30 °C): δ = 7.43 (dd, ^3J = 1.6, 7.7 Hz, 1 H, H^6), 7.02 (ddd, ^3J = 3.0, 3.0, 6.0 Hz, 1 H, H^4), 6.66 (dd, ^3J = 1.6, 7.7 Hz, 1 H, H^3), 6.51 (ddd, ^3J = 3.0, 3.0, 6.0 Hz, 1 H, H^5) ppm. ^{13}C NMR (75 MHz, $[D_6]$DMSO, 30 °C): δ = 144.69 (C^1), 130.88 (C^2), 129.72 (C^6), 127.21 (C^4), 116.04 (C^3), 115.43 (C^5) ppm. FTIR (KBr): $\tilde{\nu}$ = 3424 (m), 3370 (m), 1619 (s), 1560 (s), 1482 (s), 1317 (m), 1231 (s), 1187 (s), 1117 (m), 1065 (w), 1023 (m), 1035 (m), 826 (w), 750 (s), 709 (s), 619 (s), 576 (m), 528 (m) cm^{-1}. FTIR (Nujol): $\tilde{\nu}$ = 3320 (m), 3257 (m), 1599 (w), 1565 (w), 1296 (w), 1204 (s), 1174 (s) 1160 (m), 1131 (m), 1074 (m), 1033 (m), 1013 (s), 947 (w), 827 (m), 778 (s), 703 (s) cm^{-1}. ESI-MS^+ (solvent: DMSO/MeOH): *m*/*z* (%) = 464/466/468 (5) {triplet (1/2/1 $^{107}Ag/^{107/109}Ag/^{109}Ag$), $[Ag_2\mathbf{L}(DMSO)]^+$}; 386/388/390 (5) {triplet (1/2/1 $^{107}Ag/^{107/109}Ag/^{109}Ag$), $[Ag_2\mathbf{L}]^+$}; 263/265 (95) {doublet (1/1 $^{107}Ag/^{109}Ag$), $[Ag(\mathbf{L}–NH_2)]^+$}; 185/187 (100) {doublet (1/1 $^{107}Ag/^{109}Ag$), $[Ag(DMSO)]^+$}. $C_6H_6AgNO_3S$ (280.046): calcd. C 25.73, H 2.16, N 5.00; found C 25.57, H 2.06, N 4.87.

$[Ag(O_3SBAm)]_\infty$ (2): *m*-Aminobenzenesulfonic acid was applied to the general procedure to yield a dark purple amorphous powder

(258 mg, 92%). Recrystallization of 50 mg in water resulted in crystalline plates (55%) suitable for X-ray crystallography; m.p. > 270 °C (decomp.). ^{1}H NMR (300 MHz, [D$_6$]DMSO, 30 °C): δ = 7.03 (m, 1 H, H^5), 6.99 (s, 1 H, H^2), 6.91 (d, ^3J = 9.0 Hz, 1 H, H^6), 6.62 (m, 1 H, H^4) ppm. ^{13}C NMR (100 MHz, [D$_6$]DMSO, 30 °C): δ = 148.49 (C^1), 146.47 (C^3), 128.15 (C^5), 115.47 (C^4), 114.89 (C^6), 112.82 (C^2) ppm. FTIR (KBr): $\tilde{\nu}$ = 3432 (s), 1629 (m), 1600 (m), 1482 (m), 1452 (m), 1384 (m), 1313 (w), 1270 (w), 1188 (s), 1110 (s), 1037 (s), 992 (m), 875 (w), 791 (m), 710 (s), 691 (m), 623 (s), 562 (m), 526 (m) cm^{-1}. FTIR (Nujol): $\tilde{\nu}$ = 3362 (m), 3246 (w), 1599 (m), 1314 (w), 1254 (m), 1210 (s), 1169 (m), 1147 (s), 1108 (s), 1027 (s), 982 (m), 881 (m), 785 (m), 709 (m), 685 (m), 613 (m) cm^{-1}. ESI-MS$^+$ (solvent: DMSO/MeOH): *m*/*z* (%) = 464/466/468 (5) {triplet (1/2/1 ^{107}Ag/$^{107/109}$Ag/^{109}Ag), [Ag$_2$**L**(DMSO)]$^+$}; 386/388/390 (5) {triplet (1/2/1 ^{107}Ag/$^{107/109}$Ag/^{109}Ag), [Ag$_2$**L**]$^+$}; 313/315 (10) {doublet (1/1 ^{107}Ag/^{109}Ag), [Ag(**L**–NH$_2$)(MeOH)(H$_2$O)]$^+$}; 302/304 (5) {doublet (1/1 ^{107}Ag/^{109}Ag), [Ag**L** + Na]$^+$}; 263/265 (95) {doublet (1/1 ^{107}Ag/^{109}Ag), [Ag(**L**–NH$_2$)]$^+$}; 185/187 (100) {doublet (1/1 ^{107}Ag/^{109}Ag), [Ag(DMSO)]$^+$}; 107/109 (30){doublet (1/1), [Ag]$^+$}. C$_6$H$_6$AgNO$_3$S (280.046): calcd. C 25.73, H 2.16, N 5.00; found C 25.80, H 2.14, N 5.22.

[Ag(O$_3$SBM3A6)]$_\infty$ (3): The general procedure was followed by using 6-amino-3-methoxybenzenesulfonic acid to yield a dark purple amorphous powder (289 mg, 93%); m.p. > 150 °C (decomp.). ^{1}H NMR (300 MHz, [D$_6$]DMSO, 30 °C): δ = 7.28 (d, ^3J = 6.0 Hz, 1 H, H^3), 7.26 (s, 1 H, H^6), 7.04 (dd, ^3J = 3.0, 9.0 Hz, 1 H, H^4), 3.79 (s, 3 H, –OCH$_3$) ppm. ^{13}C NMR (100 MHz, [D$_6$]DMSO, 30 °C): δ = 158.39 (C^2), 141.78 (C^5), 125.41 (C^3), 120.08 (C^1), 115.96 (C^4), 112.21 (C^6), 55.66 (C^7) ppm. FTIR (KBr): $\tilde{\nu}$ = 3448 (s), 3079 (s), 1608 (m), 1560 (m), 1508 (m), 1492 (s), 1411 (w), 1384 (w), 1330 (m), 1252 (s), 1236 (s), 1210 (s), 1197 (s), 1132 (s), 1093 (m), 1060 (s), 1022 (s), 886 (m), 829 (m), 696 (s), 670 (w), 638 (s), 627 (s), 560 (w), 527 (m) cm^{-1}. FTIR (Nujol): $\tilde{\nu}$ = 3077 (m), 1634 (w), 1608 (w), 1494 (s), 1413 (w), 1331 (w), 1253 (s), 1237 (s), 1211 (s), 1186 (s), 1134 (m), 1095 (w), 1061 (m), 1023 (s), 888 (m), 830 (m), 697 (s), 639 (m), 629 (m) cm^{-1}. ESI-MS$^+$: (solvent: DMSO/MeOH): *m*/*z* (%) = 332/334 (10) {doublet (1/1 ^{107}Ag/^{109}Ag), [Ag**L** + Na]$^+$}; 310/312 (10) {doublet (1/1 ^{107}Ag/^{109}Ag), [Ag**L** + H]$^+$}; 122/124 (25) {doublet (1/1 ^{107}Ag/^{109}Ag), [Ag$_2$O + H]$^+$}; 107/109 (100) {doublet (1/1), [Ag]$^+$}. C$_7$H$_8$AgNO$_4$S (310.071): calcd. C 27.11, H 2.60, N 4.52; found C 27.27, H 2.81, N 5.21.

[Ag(O$_3$SNA*o*)(H$_2$O)$_{0.5}$]$_\infty$ (4a): The general procedure was carried out with *o*-amino-1-naphthalenesulfonic acid to yield pale pink crystalline needles (304 mg, 92%) suitable for X-ray crystallography; m.p. > 140 °C (decomp.). ^{1}H NMR (300 MHz, [D$_6$]DMSO, 30 °C): δ = 8.95 (d, ^3J = 6.0 Hz, 1 H, H^9), 7.96 (d, ^3J = 9.0 Hz, 1 H, H^4), 7.88 (d, ^3J = 9.0 Hz, 1 H, H^6), 7.59–7.46 (m, 2 H, H^7 and H^8), 7.29 (d, ^3J = 9.0 Hz, 1 H, H^3) ppm. ^{13}C NMR (100 MHz, [D$_6$]-DMSO, 30 °C): δ = 143.16 (C^1), 131.98 (C^2), 129.83 (C^4), 127.35 (C^{10}), 126.77 (C^6), 126.08 (C^9), 125.41 (C^5), 120.61 (C^8), 120.31 (C^7), 118.97 (C^3) ppm. FTIR (KBr): $\tilde{\nu}$ = 3430 (s), 2959 (w), 2625 (w) 1624 (s), 1559 (s), 1552 (s), 1518 (s), 1473 (m), 1427 (m), 1384 (s), 1360 (w), 1332 (w), 1233 (m), 1200 (s), 1145 (m), 1050 (s), 990 (m), 913 (w), 881 (w), 827 (w), 809 (s), 779 (m), 763 (w), 749 (w), 676 (m), 655 (m), 623 (m), 559 (m), 513 (m) cm^{-1}. FTIR (Nujol): $\tilde{\nu}$ = 3433 (w), 3342 (w), 1611 (m), 1597 (w), 1553 (m), 1503 (m), 1351 (w), 1234 (w), 1193 (s), 1146 (m), 1050 (s), 991 (m), 905 (w), 828 (w), 810 (m), 782 (m), 764 (w), 676 (m), 657 (w), 623 (m) cm^{-1}. ESI-MS$^+$ (solvent: CH_2Cl_2): *m*/*z* (%) = 520/522/524 (5) {triplet (1/2/1 ^{107}Ag/$^{107/109}$Ag/^{109}Ag), [Ag$_2$**L**(CH_2Cl_2)]$^+$}; 436/438/440 (5) {triplet (1/2/1 ^{107}Ag/$^{107/109}$Ag/^{109}Ag), [Ag$_2$**L**]$^+$}; 275/277 (5) {doublet (1/1), [Ag(CH_2Cl_2)$_2$]$^+$}; 191/193 (100) {doublet (1/1), [Ag(CH_2Cl_2)]$^+$}; 107/109 (70) {doublet (1/1), [Ag]$^+$}. $C_{10}H_9AgNO_{3.5}S$ (339.112): calcd. C 35.42, H 2.68, N 4.13; found C 32.36, H 2.60, N 3.99.

{[Ag(O$_3$SNA*o*)]·(H$_2$O)$_{0.5}$}$_\infty$ (4b): Crystalline material of **4a** (50 mg) was dissolved in EtOH and left for crystallization. After one week, pink needles were obtained [yield: 28 mg (56%)] that were suitable for X-ray crystallography. The crystals were isolated and dried in vacuo. Further analysis indicates the loss of the water molecule present in the lattice; m.p. > 160 °C (decomp.). $C_{10}H_8AgNO_3S$ (330.104): calcd. C 36.38, H 2.44, N 4.24; found C 37.57, H 2.98, N 4.53.

[Ag(O$_3$SN5A)]$_\infty$ (5): The general procedure was followed by using 5-amino-1-naphthalenesulfonic acid to yield a dark red amorphous powder (293 mg, 89%); m.p. > 220 °C (decomp.). ^{1}H NMR (300 MHz, [D$_6$]DMSO, 30 °C): δ = 8.86 (d, ^3J = 6.0 Hz, 1 H, H^9), 8.05 (d, ^3J = 9.0 Hz, 1 H, H^4), 7.95 (d, ^3J = 9.0 Hz, 1 H, H^2), 7.59 (d, ^3J = 9.0 Hz, 1 H, H^3), 7.55–7.52 (m, 2 H, H^7 and H^8) ppm. ^{13}C NMR (100 MHz, [D$_6$]DMSO, 30 °C): δ = 144.39 (C^1), 129.73 (C^6), 128.58 (C^{10}), 127.46 (C^9), 126.71 (C^5), 125.66 (C^3), 125.41 (C^4), 125.25 (C^8), 122.93 (C^2), 119.71 (C^7) ppm. FTIR (KBr): $\tilde{\nu}$ = 3469 (s), 1654 (s), 1399 (m), 1384 (m), 1350 (w), 1322 (w), 1199 (s), 1035 (s), 785 (m), 755 (w), 646 (m), 581 (m) cm^{-1}. FTIR (Nujol): $\tilde{\nu}$ = 3427 (w), 1654 (m), 1167 (s), 1027 (s), 783 (m), 645 (w), 629 (w), 582 (w) cm^{-1}. ESI-MS$^+$ (solvent: DMSO/MeOH): *m*/*z* (%) = 436/438/440 (5) {triplet (1/2/1 ^{107}Ag/$^{107/109}$Ag/^{109}Ag), [Ag$_2$L]$^+$}; 341/343 (60) {doublet (1/1 ^{107}Ag/^{109}Ag), [Ag(DMSO)$_3$]$^+$}; 263/265 (60) {doublet (1/1 ^{107}Ag/^{109}Ag), [Ag(DMSO)$_2$]$^+$}; 217/219 (10) {doublet (1/1 ^{107}Ag/^{109}Ag), [Ag(DMSO)(MeOH)]$^+$}; 185/187 (100) {doublet (1/1 ^{107}Ag/^{109}Ag), [Ag(DMSO)]$^+$}. $C_{10}H_{12}AgNO_5S$ (366.134): calcd. C 32.80, H 2.75, N 3.83; found C 32.36, H 2.72, N 3.83.

[Ag(O$_3$SN4A3H)]$_\infty$ (6): 4-Amino-3-hydroxy-1-naphthalenesulfonic acid was applied to the general procedure to yield a dark red amorphous powder (276 mg, 80%); m.p. 176–180 °C. ^{1}H NMR (300 MHz, D$_2$O, 30 °C): δ = 8.51–8.48 (m, 1 H, H^9), 8.12–8.09 (m, 1 H, H^6), 7.84 (s, 1 H, H^2), 7.56–7.52 (m, 2 H, H^7 and H^8) ppm. ^{13}C NMR [100 MHz, D$_2$O (TMS), 30 °C]: δ = 140.34 (C^3), 137.16 (C^1), 130.24 (C^4), 126.02 (C^9), 125.97 (C^{10}), 125.37 (C^7), 124.82 (C^8), 124.17 (C^5), 121.12 (C^6), 118.90 (C^2) ppm. FTIR (KBr): $\tilde{\nu}$ = 3169 (s), 1637 (s), 1607 (m), 1577 (m), 1514 (m), 1441 (s), 1400 (s), 1352 (s), 1290 (m), 1221 (s), 1196 (s), 1159 (m), 1145 (m), 1105 (m), 1081 (m), 1043 (s), 983 (w), 970 (m), 877 (m), 781 (w), 759 (m), 725 (w), 656 (m), 640 (m), 593 (s), 545 (m), 514 (m) cm^{-1}. FTIR (Nujol): $\tilde{\nu}$ = 3156 (m), 1635 (m), 1601 (m), 1576 (m), 1515 (m), 1351 (s), 1292 (m), 1197 (s), 1157 (s), 1145 (s), 1105 (m), 1042 (s), 969 (m), 946 (w), 878 (w), 760 (m), 676 (w), 657 (m), 640 (m), 594 (m) cm^{-1}. ESI-MS$^+$ (solvent: DMSO/MeOH): *m*/*z* (%) = 470/472/474 (5) {triplet (1/2/1 ^{107}Ag/$^{107/109}$Ag/^{109}Ag), [Ag$_2$**L** + H$_2$O]$^+$}; 368/370 (10) {doublet (1/1 ^{107}Ag/^{109}Ag), [Ag**L** + Na]$^+$}; 147/149 (100) {doublet (1/1 ^{107}Ag/^{109}Ag), [AgOH + Na]$^+$}. $AgC_{10}H_{12}O_6NS$ (382.131): calcd. C 31.43, H 3.17, N 3.67; found C 31.05, H 3.04, N 3.82.

[Ag(O$_3$SI)]$_\infty$ (7): The general procedure was carried out with 5-isoquinolinesulfonic acid to yield a pale yellow amorphous powder (308 mg, 98%); m.p. > 220 °C (decomp.). ^{1}H NMR (300 MHz, [D$_6$]DMSO, 30 °C): δ = 9.37 (s, 1 H, H^6), 8.71 (d, ^3J = 6.0 Hz, 1 H, H^4), 8.54 (d, ^3J = 6.0 Hz, 1 H, H^3), 8.21 (dd, ^3J = 3.0, 9.0 Hz, 1 H, H^{10}), 8.16 (d, ^3J = 9.0 Hz, 1 H, H^8), 7.69 (dd, ^3J = 3.0, 9.0 Hz, 1 H, H^9) ppm. ^{13}C NMR (100 MHz, [D$_6$]DMSO, 30 °C): δ = 153.92 (C^6), 143.17 (C^{10}), 143.10 (C^1), 131.88 (C^2), 129.46 (C^8), 129.18 (C^3), 128.68 (C^9), 126.97 (C^7), 120.90 (C^4) ppm. FTIR (KBr): $\tilde{\nu}$ = 3435 (s), 3093 (w), 3070 (w), 3026 (w), 3008 (w), 1622 (s), 1558 (s), 1569 (m), 1487 (s), 1424 (m), 1382 (w), 1369 (s), 1326 (m), 1267 (m), 1250 (s), 1218 (s), 1186 (m), 1068 (s), 1077 (m), 1055

(s), 984 (m), 934 (w), 918 (m), 842 (m), 814 (s), 802 (m), 751 (s), 709 (s), 629 (s), 575 (s), 537 (m), 515 (s), 466 (m), 426 (m), 410 (m) cm^{-1}. FTIR (Nujol): $\tilde{\nu}$ = 3437 (s), 3351 (s), 3094 (m), 1623 (s), 1591 (m), 1561 (w), 1487 (m), 1320 (w), 1274 (m), 1210 (s), 1175 (s), 1056 (s), 988 (m), 969 (w), 956 (w), 944 (w), 926 (w), 843 (m), 831 (m), 814 (m), 763 (s), 705 (m), 624 (m) cm^{-1}. ESI-MS^+ (DMSO/MeOH): *m*/*z* (%) = 373/375 (10) {doublet (1/1 $^{107}Ag/^{109}Ag$), $[AgL(LH)(DMSO)_2(MeOH)_2 + 2H]^{2+}$}; 368/370/372 (5) {triplet (1/2/1 $^{107}Ag/^{107/109}Ag/^{109}Ag$), $[Ag_2L(LH)(MeOH)_2(H_2O) + Na]^{2+}$}; 356/358 (5) {doublet (1/1 $^{107}Ag/^{109}Ag$), $[AgL(H_2O) + Na]^+$}; 341/343 (80) {doublet (1/1 $^{107}Ag/^{109}Ag$), $[AgL(LH)(DMSO)_2 + 2H]^{2+}$}; 317/319 (40) {doublet (1/1 $^{107}Ag/^{109}Ag$), $[AgL(LH)(H_2O)_6 + 2H]^{2+}$}; 295/297 (15) {doublet (1/1 $^{107}Ag/^{109}Ag$), $[AgL(LH)(MeOH)_2 + 2H]^{2+}$}; 290/2920 (50) {doublet (1/1 $^{107}Ag/^{109}Ag$), $[AgL(LH)(H_2O)_3 + 2H]^{2+}$}; 263/265 (100) {$[AgL(LH) + 2H]^{2+}$}. $C_9H_8AgNO_4S$ (334.093): calcd. C 32.35, H 2.41, N 4.19; found C 32.03, H 2.40, N 4.15.

$[Ag(O_3SBAp)]_\infty$ (8): The general procedure was carried out with *p*-aminobenzenesulfonic acid as ligand to yield amber crystalline blocks (278 mg, 99%) suitable for X-ray crystallography; m.p. > 250 °C (decomp.). ^1H NMR (300 MHz, [D$_6$]DMSO, 30 °C): δ = 7.33 (d, ^3J = 8.6 Hz, 2 H, H^2 and H^6), 6.58 (d, ^3J = 6.4 Hz, 2 H, H^3 and H^5) ppm. ^{13}C NMR (75 MHz, [D$_6$]DMSO, 30 °C): δ = 149.91 (C^1), 135.56 (C^4), 127.72 (C^2 and C^6), 114.66 (C^3 and C^5) ppm. FTIR (KBr): $\tilde{\nu}$ = 3469 (m), 3320 (s), 3268 (s), 3185 (s), 1905 (w), 1600 (s), 1498 (s), 1437 (s), 1332 (w), 1298 (w), 1248 (m), 1197 (s), 1183 (s), 1152 (s), 1124 (s), 1032 (s), 1000 (s), 945 (s), 841 (m), 826 (s), 692 (s), 568 (s) cm^{-1}. FTIR (Nujol): $\tilde{\nu}$ = 3319 (m), 3267 (m), 3184 (m), 1714 (w), 1599 (m) 1498(m), 1304 (w), 1249 (w), 1186 (s), 1153 (s), 1123 (s), 991 (s), 946 (m), 843 (w), 827 (m), 691 (m), 569 (s) cm^{-1}. ESI-MS^+ (solvent: DMSO/MeOH): *m*/*z* (%) = 944/946/948/950/952 (5) {quintet (1/4/6/4/1 $^{107}Ag/^{3\times107/109}Ag/^{3\times109/107}Ag/^{2\times107/2\times109}Ag/^{109}Ag$), $[Ag_4L_3]^+$}; 743/745/747/749 (5) {quartet (1/3/3/1 $^{107}Ag/^{2\times107/109}Ag/^{2\times109/107/109}Ag$), $[Ag_3L_2(DMSO)]^+$}; 665/667/669/671 (5) {quartet (1/3/3/1 $^{107}Ag/^{2\times107/109}Ag/^{2\times109/107/109}Ag$), $[Ag_3L_2]^+$}; 542/544/546 (5) {triplet (1/2/1 $^{107}Ag/^{107/109}Ag/^{109}Ag$), $[Ag_2L(DMSO)_2]^+$}; 464/466/468 (10) {triplet (1/2/1 $^{107}Ag/^{107/109}Ag/^{109}Ag$), $[Ag_2L(DMSO)]^+$}; 263/265 (15) {doublet (1/1 $^{107}Ag/^{109}Ag$), $[Ag(L–NH_2)]^+$}; 185/187 (100) {doublet (1/1 $^{107}Ag/^{109}Ag$), $[Ag(DMSO)]^+$}; 107/109 (30) {doublet (1/1), $[Ag]^+$}. $C_6H_6AgNO_3S$ (280.046): calcd. C 25.73, H 2.16, N 5.00; found C 25.86, H 2.20, N 4.78.

$[Ag(O_3SP)]_\infty$ (9): 2-Pyridinesulfonic acid was applied to the general procedure to yield colourless crystalline blocks (264 mg, 99%) suitable for X-ray crystallography; m.p. > 245 °C (decomp.). ^1H NMR (300 MHz, [D$_6$]DMSO, 30 °C): δ = 8.60 (d, ^3J = 3.0 Hz, 1 H, H^3), 8.05 (td, ^3J = 3.0, 9.0 Hz, 1 H, H^5), 7.95 (d, ^3J = 9.0 Hz, 1 H, H^6), 7.58 (m, 1 H, H^4) ppm. ^{13}C NMR (100 MHz, [D$_6$]DMSO, 30 °C): δ = 162.18 (C^1), 149.91 (C^5), 139.53 (C^3), 125.24 (C^4), 121.35 (C^6) ppm. FTIR (KBr): $\tilde{\nu}$ = 3422 (m), 1617 (w), 1579 (m), 1458 (m), 1425 (m), 1291 (w), 1208 (s), 1164 (m), 1093 (m), 1049 (m), 1040 (m), 994 (m), 777 (m), 747 (m), 645 (s), 618 (m), 566 (m), 556 (m) cm^{-1}. FTIR (Nujol): $\tilde{\nu}$ = 3394 (w), 1634 (w), 1584 (w), 1429 (m), 1294 (w), 1256 (m), 1232 (m), 1207 (s), 1165 (s), 1146 (s), 1094 (m), 1049 (s), 1019 (m), 1005 (m), 7778 (m), 736 (m), 628 (m) cm^{-1}. ESI-MS^+ (solvent: CH_2Cl_2): *m*/*z* (%) = 456/458/460 (5) {triplet (1/2/1 $^{107}Ag/^{107/109}Ag/^{109}Ag$), $[Ag_2L(CH_2Cl_2)]^+$}; 372/374/376 (10) {triplet (1/2/1 $^{107}Ag/^{107/109}Ag/^{109}Ag$), $[Ag_2L]^+$}; 191/193 (100) {doublet (1/1 $^{107}Ag/^{109}Ag$), $[Ag(CH_2Cl_2)]^+$}; 107/109 (60) {doublet (1/1), $[Ag]^+$}. $C_5H_4AgNO_3S$ (266.022): calcd. C 22.57, H 1.52, N 5.27; found C 22.77, H 1.40, N 5.22.

X-ray Crystallography: Crystalline samples of **1**, **2**, **4a** and **4b** were mounted onto a glass fibre in viscous hydrocarbon oil. Crystal data were collected with either an Enraf–Nonius Kappa CCD or a Bruker X8 APEX CCD instrument with monochromated Mo-K_α radiation, λ = 0.71073 Å. All data were collected at 123 K, maintained using an open flow of nitrogen from an Oxford Cryostreams cryostat. X-ray data were processed with the DENZO program.[15] Structural solution and refinement was carried out using SHELXL-97[16] with the graphical interface X-Seed.[17] Data were corrected for absorption using the SADABS[18] package. The refinements were carried out by using full-matrix least-squares techniques on F^2, minimizing the function $(F_o - F_c)^2$, for which the weight is defined as $4F_o^2/2F_{o(2)}$ and F_o and F_c are the observed and calculated structure factor amplitudes using the program SHELXL-97.[16] During the refinement of **2**, the Flack parameter

Table 4. Crystallographic data and structure refinement for compounds **1**, **2**, **4a** and **4b**.

	1	**2**	**4a**	**4b**
Formula	$C_6H_6AgNO_3S$	$C_6H_6AgNO_3S$	$C_{10}H_{10}AgNO_4S$	$C_{10}H_8AgNO_3S{\cdot}H_2O$
M_r	280.05	280.05	348.12	348.12
Crystal size [mm]	0.28 × 0.16 × 0.13	0.42 × 0.26 × 0.23	0.21 × 0.23 × 0.15	0.45 × 0.15 × 0.30
Crystal system	monoclinic	orthorhombic	monoclinic	monoclinic
Space group	$P2_1/c$ (no. 14)	$P2_12_12_1$ (no. 19)	$P2_1$ (no. 4)	$C2/c$ (no. 15)
a [Å]	5.5730(11)	5.7400(11)	7.2689(15)	22.4750(5)
b [Å]	17.435(4)	8.3240(17)	7.5693(15)	7.4410(15)
c [Å]	7.8510(16)	16.477(3)	9.6200(19)	14.5490(3)
α [°]	90	90	90	90
β [°]	108.43(3)	90	104.48(3)	123.05(3)
γ [°]	90	90	90	90
V [Å^3]	723.7(3)	787.3(3)	512.47(18)	2039.4(10)
Z	4	4	2	8
T [K]	123(2)	123(2)	123(2)	123(2)
$\rho_{calcd.}$ [g cm^{-1}]	2.570	2.363	2.256	2.268
μ [mm^{-1}]	3.030	2.785	2.171	2.182
Reflections collected/unique	7215/1713	22987/3402	2423/2037	28377/3861
Flack *x*	–	0.50(2)	0.18(6)	–
R_{int}	0.0593	0.0394	0.0528	0.0371
*R*1 [$I > 2\sigma(I)$]	0.0368	0.0315	0.0580	0.0335
*wR*2 (all data)	0.0909	0.0467	0.1417	0.0598
GoF	1.177	1.059	1.059	1.084

was 0.5, which was not due to missing symmetry. Therefore the data was refined as a racemic twin. The final values of refinement parameters are given in Table 4.

CCDC-848459 (for **1**), -848460 (for **2**), -848461 (for **4a**) and -848462 (for **4b**) contain the supplementary crystallographic data for this paper. These data can be obtained free of charge from The Cambridge Crystallographic Data Centre via www.ccdc.cam.ac.uk/data_request/cif.

Acknowledgments

We thank the Australian Research Council and Monash University for funding.

[1] a) U. S. Agarwal, S. Thampi, A. K. Jain, Reliance Industries Limited, India, **2009**, PCT Int. Appl. WO 2009072144; b) D. Baram-Pinto, S. Shukla, N. Perkas, A. Gedanken, R. Sarid, *Bioconjugate Chem.* **2009**, *20*, 1497–1502; c) X. Cao, M. Tang, F. Liu, Y. Nie, C. Zhao, *Colloids Surf. B: Biointerfaces* **2010**, *81*, 555–562; d) T. Kawakami, S. Teshima, Y. Asako, H. Tsuboi, Nippon Shokubai Kagaku Kogyo Co., Ltd., Japan, **1997**, Jpn. Kokai Tokkyo Koho JP 09301812; e) K. Shirai, Y. Ishii, S. Nomura, S. Shoji, O. Suzuki, T. Sato, Nippi Inc., Japan, **2002**, Jpn. Kokai Tokkyo Koho JP 2002220311; f) L. Stephen, Specialty Fibres and Materials Limited, UK, **2010**, PCT Int. Appl. WO 2010061225; g) D. Vachon, G. E. Wnek, Aegis Biosciences, LLC, USA, **2001**, US Pat. Appl. US 6306419; h) K. Vasilev, V. R. Sah, R. V. Goreham, C. Ndi, R. D. Short, H. J. Griesser, *Nanotechnology* **2010**, *21*, 215102/1–215102/6.

[2] a) A. P. Cote, M. J. Ferguson, K. A. Khan, G. D. Enright, A. D. Kulynych, S. A. Dalrymple, G. K. H. Shimizu, *Inorg. Chem.* **2002**, *41*, 287; b) A. P. Cote, G. K. H. Shimizu, *Inorg. Chem.* **2004**, *43*, 6663–6673; c) D. J. Hoffart, S. A. Dalrymple, G. K. H. Shimizu, *Inorg. Chem.* **2005**, *44*, 8868–8875; d) S. K. Makinen, N. J. Melcer, M. Parvez, G. K. H. Shimizu, *Chem. Eur. J.* **2001**, *7*, 5176; e) G. K. H. Shimizu, G. D. Enright, C. I. Ratcliffe, K. F. Preston, J. L. Reid, J. A. Ripmeester, *Chem. Commun.* **1999**, 1485–1486; f) G. K. H. Shimizu, G. D. Enright, C. I. Ratcliffe, G. S. Rego, J. L. Reid, J. A. Ripmeester, *Chem. Mater.* **1998**, *10*, 3282–3283; g) G. K. H. Shimizu, G. D. Enright, C. I. Ratcliffe, J. A. Ripmeester, *Chem. Commun.* **1999**, 461–462; h) G. Smith, B. A. Cloutt, D. E. Lynch, K. A. Byriel, C. H. L. Kennard, *Inorg. Chem.* **1998**, *37*, 3236–3242; i) F. Charbonnier, R. Faure, H. Loiseleur, *Cryst. Struct. Commun.* **1981**, *10*, 1129; j) C.-H. Chen, J.-W. Cai, X.-L. Feng, X.-M. Chen, *Polyhedron* **2002**, *21*, 689; k) G. Smith, J. H. Thomasson, J. M. White, *Aust. J. Chem.* **1999**, *52*, 317; l) N. J. Melcer, G. D. Enright, J. A. Ripmeester, G. K. H. Shimizu, *Inorg. Chem.* **2001**, *40*, 4641; m) G. K. H. Shimizu, G. D. Enright, G. S. Rego, J. A. Ripmeester, *Can. J. Chem.* **1999**, *77*, 313; n) J.-F. Ma, J. Yang, S.-L. Li, S.-Y. Song, H.-J. Zhang, H.-S. Wang, K.-Y. Yang, *Cryst. Growth Des.* **2005**, *5*, 807; o) A. D. Kulynych, G. K. H. Shimizu, *CrystEngComm* **2002**, *18*, 102; p) G. Wulfsberg, K. D. Parks, R. Rutherford, D. J. Jackson, F. E. Jones, D. Derrick, W. Ilsley, S. H. Strauss, S. M. Miller, O. P. Anderson, T. A. Babushkina, S. I. Gushchin, E. A. Kravchenko, V. G. Morgunov, *Inorg. Chem.* **2002**, *41*, 2032; q) D. Sun, R. Cao, Y. Liang, M. Hong, *Chem. Lett.* **2002**, 198; r) D. Sun, R. Cao, Y. Sun, W. Bi, X. Li, M. Hong, Y. Zhao, *Eur. J. Inorg. Chem.* **2003**, 38; s) D. Sun, R. Cao, W. Bi, X. Li, Y. Wang, M. Hong, *Eur. J. Inorg. Chem.* **2004**, 2144; t) L. J. May, G. K. H. Shimizu, *Chem. Mater.* **2005**, *17*, 217; u) P. F. Charbonnier, *Acta Crystallogr. Sect. B: Struct. Crystallogr. Cryst. Chem.* **1977**, *33*, 2824; v) P. F. Charbonnier, R. F. H. Loiseleur, *Acta Crystallogr. Sect. B: Struct. Crystallogr. Cryst. Chem.* **1978**, *34*, 3598; w) P. F. Charbonnier, R. F. H. Loiseleur, *Acta Crystallogr. Sect. B: Struct. Crystallogr. Cryst. Chem.* **1979**, *35*, 1773; x) M. Sebastian, H. K. Y. John, J. V. Jagadese, *J. Chem. Soc. Dalton Trans.* **2002**, 4561.

[3] a) X.-H. Bu, H. Liu, M. Du, K. M.-C. Wong, V. W.-W. Yam, M. Shionoya, *Inorg. Chem.* **2001**, *40*, 4143; b) Y.-B. Dong, J.-Y. Cheng, R.-Q. Huang, *Inorg. Chem.* **2003**, *42*, 5699; c) Y.-B. Dong, J.-P. Ma, R.-Q. Huang, *Inorg. Chem.* **2003**, *42*, 294; d) R. P. Feazell, C. E. Carson, K. Klausmeyer, *Inorg. Chem.* **2006**, *45*, 2635; e) K. A. Hirsch, S. R. Wilson, J. S. Moore, *Inorg. Chem.* **1997**, *36*, 2960; f) C. Kaes, M. W. Hosseini, C. E. F. Rickard, B. W. Skelton, A. H. White, *Angew. Chem.* **1998**, *110*, 970; *Angew. Chem. Int. Ed.* **1998**, *37*, 920; g) F.-F. Li, J.-F. Ma, S.-Y. Song, J. Yang, H.-Q. Jia, N.-H. Hu, *Cryst. Growth Des.* **2006**, *6*, 209; h) F.-F. Li, J.-F. Ma, S.-Y. Song, J. Yang, Y.-Y. Liu, Z.-M. Su, *Inorg. Chem.* **2005**, *44*, 9374–9383; i) F.-F. Li, J.-F. Ma, J. Yang, H.-Q. Jia, N.-H. Hu, *THEOCHEM* **2006**, *787*, 106; j) C.-S. Liu, P.-Q. Chen, E.-C. Yang, J.-L. Tian, X.-H. Bu, Z.-M. Li, H.-W. Sun, Z. Lin, *Inorg. Chem.* **2006**, *45*, 5812; k) H.-Y. Liu, H. Wu, J.-F. Ma, S.-Y. Song, J. Yang, Y.-Y. Liu, Z.-M. Su, *Inorg. Chem.* **2007**, *46*, 7299; l) H.-Y. Liu, H. Wu, J.-F. Ma, J. Yang, Y.-Y. Liu, *Dalton Trans.* **2009**, 7957–7968; m) K. Matsumoto, Y. Harada, N. Yamada, H. Kurata, T. Kawase, M. Oda, *Cryst. Growth Des.* **2006**, *6*, 1083; n) G. Smith, B. A. Cloutt, K. A. Byriel, C. H. L. Kennard, *Aust. J. Chem.* **1997**, *50*, 741; o) G. Smith, D. E. Lynch, C. H. L. Kennard, *Inorg. Chem.* **1996**, *35*, 2711; p) D. Sun, R. Cao, Y. Sun, W. Bi, X. Li, Y. Wang, Q. Shi, X. Li, *Inorg. Chem.* **2003**, *42*, 7512; q) H. Wu, X.-W. Dong, H.-Y. Liu, J.-F. Ma, S.-L. Li, J. Yang, Y.-Y. Liu, Z.-M. Su, *Dalton Trans.* **2008**, 5331–5341; r) S.-P. Yang, X.-M. Chen, L.-N. Ji, *J. Chem. Soc. Dalton Trans.* **2000**, 2337.

[4] Y. Jimbo, E. Takahashi, Y. Shimada, K. Sato, Fujifilm Corporation, Japan, **2008**, Eur. Pat. Appl. EP 1889601.

[5] a) J. Ibata, Y. Shimamura, Asahi Chemical Industry Co., Ltd., Japan, **1989**, Jpn. Kokai Tokkyo Koho JP 01274129; b) R. A. Lee, du Pont de Nemours, E. I., and Co., USA, **1985**, US Pat. Appl. US 4504575.

[6] a) B. D. Chandler, A. P. Cote, D. T. Cramb, J. M. Hill, G. K. H. Shimizu, *Chem. Commun.* **2002**, 1900; b) A. P. Cote, G. K. H. Shimizu, *Chem. Commun.* **2001**, 251; c) A. P. Cote, G. K. H. Shimizu, *Coord. Chem. Rev.* **2003**, *245*, 49–64; d) A. P. Cote, G. K. H. Shimizu, *Chem. Eur. J.* **2003**, *9*, 5361; e) S. A. Dalrymple, M. Parvez, G. K. H. Shimizu, *Chem. Commun.* **2001**, 2672; f) S. A. Dalrymple, M. Parvez, G. K. H. Shimizu, *Inorg. Chem.* **2002**, *41*, 6986; g) S. A. Dalrymple, G. K. H. Shimizu, *Chem. Commun.* **2002**, 2224; h) S. A. Dalrymple, G. K. H. Shimizu, *Chem. Eur. J.* **2002**, *8*, 3010; i) D. J. Hoffart, A. P. Cote, G. K. H. Shimizu, *Inorg. Chem.* **2003**, *42*, 8603; j) D. S. Reddy, S. Duncan, G. K. H. Shimizu, *Angew. Chem.* **2003**, *115*, 1398; *Angew. Chem. Int. Ed.* **2003**, *42*, 1360; k) J. O. Yu, A. P. Cote, G. D. Enright, G. K. H. Shimizu, *Inorg. Chem.* **2001**, *40*, 582; l) G. K. H. Shimizu, R. Vaidhyanathan, J. M. Taylor, *Chem. Soc. Rev.* **2009**, *38*, 1430–1449.

[7] a) J. Cai, *Coord. Chem. Rev.* **2004**, *248*, 1061–1083; b) J. Cai, C.-H. Chen, C.-Z. Liao, J.-H. Yao, X.-P. Hu, X.-M. Chen, *J. Chem. Soc. Dalton Trans.* **2001**, 1137; c) J. W. Cai, C. H. Chen, X. L. Feng, C. Z. Liao, X. M. Chen, *J. Chem. Soc. Dalton Trans.* **2001**, 2370; d) J. W. Cai, C. H. Chen, C. Z. Liao, X. L. Feng, X. M. Chen, *Acta Crystallogr. Sect. B* **2001**, *57*, 520; e) J. W. Cai, J. S. Zhou, M. L. Lin, *J. Mater. Chem.* **2003**, *13*, 1806; f) J.-W. Cai, C.-H. Chen, J.-S. Zhou, *Chin. J. Inorg. Chem.* **2003**, *19*, 81; g) J.-W. Cai, J.-S. Zhou, M.-L. Lin, *J. Mater. Chem.* **2003**, *13*, 1906; h) C. H. Chen, J. W. Cai, C. Z. Liao, X. L. Feng, X. M. Chen, S. W. Ng, *Inorg. Chem.* **2002**, *41*, 4967; i) J.-S. Zhou, J. Cai, L. Wang, *Dalton Trans.* **2004**, 1493.

[8] a) J. L. Atwood, L. J. Barbour, M. J. Hardie, C. L. Raston, *Coord. Chem. Rev.* **2001**, *222*, 3; b) R. Custelcean, M. D. Ward, *Angew. Chem.* **2002**, *114*, 1800; *Angew. Chem. Int. Ed.* **2002**, *41*, 1724; c) K. T. Holman, A. M. Pivovar, J. A. Swift, M. D. Ward, *Acc. Chem. Res.* **2001**, *34*, 107; d) M. J. Horner, K. T. Holman, M. D. Ward, *Angew. Chem.* **2001**, *113*, 4169; *Angew.*

Chem. Int. Ed. **2001**, *40*, 4045; e) A. R. Kennedy, M. P. Hughes, M. L. Monaghan, E. Staunton, S. J. Teat, W. E. Smith, *J. Chem. Soc. Dalton Trans.* **2001**, 2199; f) G. Mezei, R. G. Rapris, *New J. Chem.* **2003**, *27*, 1399; g) S. H. Park, C. E. Lee, *Chem. Commun.* **2003**, 1838; h) J. A. Swift, M. D. Ward, *Chem. Mater.* **2000**, *12*, 1501; i) X.-L. Zhang, B.-H. Ye, X.-M. Chen, *Cryst. Growth Des.* **2005**, *5*, 1609; j) A. Mietrach, T. W. T. Muesmann, J. Christoffers, M. S. Wickleder, *Eur. J. Inorg. Chem.* **2009**, 5328–5334; k) A. Mietrach, T. W. T. Muesmann, C. Zilinski, J. Christoffers, M. S. Wickleder, *Z. Anorg. Allg. Chem.* **2011**, *637*, 195–200; l) T. W. T. Muesmann, A. Mietrach, J. Christoffers, M. S. Wickleder, *Z. Anorg. Allg. Chem.* **2010**, *636*, 1307–1312; m) T. W. T. Muesmann, C. Zitzer, A. Mietrach, T. Kluener, J. Christoffers, M. S. Wickleder, *Dalton Trans.* **2011**, *40*, 3128–3141; n) T. W. T. Muesmann, C. Zitzer, M. S. Wickleder, J. Christoffers, *Inorg. Chim. Acta* **2011**, *369*, 45–48.

[9] a) G. Alberti, U. Constantino, in: *Inclusion Compounds*. (Eds.: J. L. Atwood, J. E. D. Davis, D. D. MacNicol), Oxford University Press, New York, **1991**, vol. 5, p. 136; b) G. Alberti, U. Constantino in *Comprehensive Supramolecular Chemistry* (Eds.: G. Alberti, T. Bein), Elsevier Science, New York, **1996**, vol. 7; c) A. Clearfield, *Prog. Inorg. Chem.* **1998**, *47*, 371; d) C. P. Johnson, J. L. Atwood, J. W. Steed, C. B. Bauer, R. D. Rogers, *Inorg. Chem.* **1996**, *35*, 2602; e) E. J. Kosnic, E. L. McClymont, R. A. Hodder, P. J. Squattrito, *Inorg. Chim. Acta* **1992**, *201*, 143.

[10] a) B. F. Abrahams, M. J. Hardie, B. F. Hoskins, R. Robson, G. A. Williams, *J. Am. Chem. Soc.* **1992**, *114*, 10641; b) K. Biradha, M. Fujita, *Angew. Chem.* **2002**, *114*, 3542; *Angew. Chem. Int. Ed.* **2002**, *41*, 3392; c) K. Biradha, Y. Hongo, M. Fujita, *Angew. Chem.* **2002**, *114*, 3545; *Angew. Chem. Int. Ed.* **2002**, *41*, 3395; d) C. J. Kepert, T. J. Prior, M. J. Rosseinsky, *J. Am. Chem. Soc.* **2000**, *122*, 5158; e) Z.-X. Lian, J. Cai, C.-H. Chen, *Polyhedron* **2007**, *26*, 2647–2654; f) D. V. Soldatov, J. A. Ripmeester, S. I. Shergina, I. E. Sokolov, A. S. Zanina, S. A. Gromilov, Y. A. Dyadin, *J. Am. Chem. Soc.* **1999**, *121*, 4179; g) D. V. Soldatov, P. Tinnemans, G. D. Enright, C. I. Ratcliffe, P. R. Diamente, J. A. Ripmeester, *Chem. Mater.* **2003**, *15*, 3826; h) L. C. Tabares, J. A. R. Navarro, J. M. Salas, *J. Am. Chem. Soc.* **2001**, *123*, 393; i) K. Uemura, S. Kitagawa, K. Fukui, K. Saito, *J. Am. Chem. Soc.* **2004**, *126*, 3817; j) K. Uemura, S. Kitagawa, M. Kondo, K. Fukui, R. Kitaura, H. C. Chang, T. Mizutani, *Chem. Eur. J.* **2002**, *8*, 3586; k) J. J. Vittal, X. Yang, *Cryst. Growth Des.* **2002**, *2*, 259.

[11] a) Z.-P. Deng, L.-H. Huo, M.-S. Li, L.-W. Zhang, Z.-B. Zhu, H. Zhao, S. Gao, *Cryst. Growth Des.* **2011**, *11*, 3090–3100; b) Z.-P. Deng, M.-S. Li, Z.-B. Zhu, L.-H. Huo, H. Zhao, S. Gao, *Organometallics* **2011**, *30*, 1961–1967; c) Z.-P. Deng, Z.-B. Zhu, S. Gao, L.-H. Huo, H. Zhao, *Dalton Trans.* **2009**, *38*, 1290–1292; d) Z.-P. Deng, Z.-B. Zhu, S. Gao, L.-H. Huo, H. Zhao, S. W. Ng, *Dalton Trans.* **2009**, *38*, 6552–6561.

[12] a) A. Leon, *Historia Natural das Doencas Mexico, Mexico* **1992**, *Centro de Documentacion Institucional*, p. 782; b) Y.-J. Pan, F.-J. Meng, X.-J. Wang, H.-L. Zhu, D.-Q. Wang, *Z. Kristallogr. New Cryst. Struct.* **2003**, *218*, 253–254; c) J. Schreuer, *Z. Kristallogr. New Cryst. Struct.* **1999**, *214*, 311–312; d) O. Sadeghi, M. M. Amini, S. W. Ng, *Acta Crystallogr. Sect. E Struct. Rep. Online* **2010**, *66*, m855–m856; e) F. R. Ahmed, D. W. J. Cruickshank, *Acta Crystallogr.* **1952**, *5*, 852.

[13] M. Tanabe, R. H. Peters, *Org. Synth. Coll. Vol.* **1990**, 7.

[14] J. W. Steed, J. L. Atwood, *Supramolecular Chemistry*, Wiley, Toronto, **2000**, p. 19.

[15] Z. Otwinowski, W. Minor, *Methods Enymol.* **1997**, *276*, 307.

[16] G. M. Sheldrick, *Acta Crystallogr. Sect. A* **2008**, *64*, 112.

[17] L. J. Barbour, *XSEED: A graphical interface for use with the SHELX97 program suite*, University of Missouri, USA, **1999**.

[18] G. M. Sheldrick, *SADABS, Program for area detector adsorption correction*, Institute for Inorganic Chemistry, University of Göttingen, Germany, **1996**.

Received: October 14, 2011
Published Online: January 31, 2012

